



High Resolution Land Surface Modelling over Africa: the role of uncertain soil properties in combination with temporal model resolution.

Bamidele Oloruntoba^{1,2}, Stefan Kollet^{1,2}, Carsten Montzka¹, Harry Vereecken^{1,2}, Harrie-Jan
5 Hendricks Franssen^{1,2}

¹ Forschungszentrum Jülich, Institute of Bio- and Geosciences: Agrosphere (IBG-3), 52425 Jülich, Germany

² Centre for High-Performance Scientific Computing in Terrestrial Systems, Geoverbund ABC/J, 52425 Jülich,,
Germany.

Correspondence to: Bamidele Oloruntoba (b.oloruntoba@fz-juelich.de)

10 **Abstract.** Land surface modelling runs with CLM5 over Africa at 3km resolution were carried out and we
assessed the impact of different sources of soil information and different upscaling strategies of the soil
information, also in combination with different atmospheric forcings and different temporal resolutions of those
atmospheric forcings. FAO and SoilGrids250m were used as soil information. SoilGrids information at 250m
15 SoilGrids250m grid cells contained in the model grid cell; (ii) arithmetic averaging of SoilGrids soil texture values
and (iii) selection of the dominant soil texture. These different soil model inputs were combined with different
atmospheric forcing model inputs, which provide inputs at different temporal resolutions: CRUNCEPv7 (6-hourly
input resolution), GSWPv3 (3-hourly) and WFDE5 (hourly). We found that varying the source of soil texture
information (FAO or SoilGrids250m) influences model water balance outputs more than the upscaling
20 methodology of the soil texture maps. However, for high temporal resolution of atmospheric forcings (WFDE5)
the different soil texture upscaling methods result in large differences in simulated evapotranspiration, surface
runoff and subsurface runoff at the local and regional scales related to the higher temporal resolution
representation of rainfall intensity in the model. The upscaling methodology of fine scale soil texture information
influences land surface model simulation results, but only clearly in combination with high temporal resolution
25 atmospheric forcings.

1. Introduction

Understanding the intricate dynamics of land surface models (LSMs) over Africa involves a detailed examination
of soil properties, which are indispensable yet steeped with uncertainty. The heterogeneity and complexity of soil
30 properties (Vågen et al., 2016; Hengl et al., 2021) influence LSM simulations (Li et al., 2022), yet they often
remain inadequately described within LSMs (Xu et al., 2023) due to limited data availability as a result of spatially
insufficient measurements (Dube et al., 2023). This inadequacy is further exacerbated in LSMs by the need to
represent the point scale measurements at a coarse spatial resolution for field, regional or continental scale studies.



35 Consequently, upscaling of soil information becomes a critical undertaking, aiming to bridge the gap between the fine-scale variability of soil properties and the broader scale at which LSMs usually operate (Van Looy et al., 2017; Montzka et al., 2017).

40 Quality of input datasets, like atmospheric forcings, soil physical properties or land surface parameters were found to greatly impact land surface modelling. Vahmani & Hogue (2014) compared remotely sensed green vegetation fraction (GVF) and impervious surface area (ISA) with the default look-up table derived values of the same parameter. The authors found that using the remotely sensed parameters, the model was able to replicate the observed ET. The achievement was attributed to capturing all year-round irrigation by the remotely sensed data in the domain of interest. This highlights the importance of the source of input datasets into LSMs. The sensitivity of land surface models to atmospheric forcings as exemplified by Traore et al. (2014) over Africa was analyzed with just two atmospheric forcing datasets; Watch Forcing Data Era Interim (WFDEI) and Watch Forcing Data 45 (WFD). These two reanalysis datasets were generated using the same methodologies but with a slight difference in their source datasets (Weedon et al., 2014) and results show that although there is a poor performance of ET in Central African forests, WFDEI was closer to eddy covariance measurements than WFD with correlations between 0.25 and 0.40. Lovat et al. (2019) used the ISBA-TOP coupled system (Bouilloud et al., 2010) over locations in the Mediterranean region at varying resolutions to assess river discharge and spatial runoff. It was noted that soil texture influences river discharge and runoff more than land cover does. Tafasca et al. (2019) used the land surface model ORCHIDEE and various global soil texture maps and noted that SoilGrids1km upscaled to 0.5o by selecting the dominant soil type generated similar water budgets as the 5 arc-min FAO Soil Map of The World (Reynolds et al., 2000) and the 1o resolution Global Soil Types map of Zobler (1986). The authors however indicated that the weak model sensitivity to the soil texture variation could have been caused by the coarse spatial 55 resolution of 0.5o at which soil texture was discretized in the ORCHIDEE model.

In this work, we are concerned with understanding the role of high-resolution soil texture input (at 3km horizontal spatial resolution) and its upscaling in the Community Land Model version 5.0 (CLM5.0) simulations over the entire African continent. This study investigates the impact of uncertainty in soil input variables and the upscaling method of soil texture information, at different spatial scales (from local to continental), and also in 60 combination with different temporal resolutions of atmospheric forcings. The aim is not to compare simulations with measurements, but to detect model-internal sensitivities to (the upscaling of) soil texture information.

For soil texture IGBP-DIS (Global Soil Data Task, 2014) hereafter “FAO” and SoilGrids250m (Hengl et al., 2017) were used as input. SoilGrids250m has a spatial resolution of 250m and is therefore considered because of its potential to better represent local scale soil processes related to the higher spatial resolution. When evaluated 65 with soil profiles from WoSIS (World Soil Information Service), SoilGrids250m has a higher accuracy than FAO with a RMSE of 18.6% versus 26.3% for the sand fraction at 0-30cm depth and 12.5% versus 15.4% for clay fractions at this depth (Dai et al., 2019). The SoilGrids250m dataset is upscaled from 250m to the model grid resolution of 3km according three different methods to reflect the uncertainties associated with the upscaling process.

70 In this study CRUNCEPv7 (Viovy, 2018), GSWP3 (Hyungjun, 2017) and WFDE5 (the bias corrected ERA5 dataset using WATCH Forcing Data methodology) (Cucchi et al., 2020) were used as meteorological forcing



75 datasets. These three forcings have been selected because of physical consistency between the input variables for the land surface model, consistency of their spatial resolution and, especially, their varying temporal resolution of 6 hours (CRUNCEP), 3 hours (GSWP) and 1 hour (WFDE5). The varying temporal resolution was investigated to study its impact in combination with the different soil texture inputs. GSWPv3 and CRUNCEPv7 have been used in the past already in combination with CLM4, CLM4.5 and CLM5 (Bonan et al., 2019). WFDE5 has been tested at 13 globally spread FLUXNET2015 locations. Cucchi et al. (2020) showed that WFDE5 has smaller mean absolute errors and larger correlations of variables like precipitation, global radiation, specific humidity, air temperature, and wind speed with observations than the WFDEI (Watch Forcing data ERA Interim) dataset which was used in Traore et al. (2014) over Africa.

80 Twelve simulations combining the four soil texture inputs (FAO and three differently upscaled SoilGrid maps) and the three meteorological forcings were carried out and results are analysed in this work at the continental, regional and point scale. The novelty of this work lies in the detection of the impact of uncertainty in the (upscaling of) soil texture information, especially in combination with different temporal resolutions of atmospheric forcings. The impact of uncertainties of atmospheric forcings on land surface model simulations over Africa has been studied but its interaction with the uncertainties in soil information has not been studied over Africa at a high spatial resolution.

85 This research therefore seeks to answer the following questions: 1) Are simulation results of CLM5.0 sensitive to different soil texture inputs, and different upscaling methods applied to soil texture input?; 2) What is the role of the temporal resolution of atmospheric forcings in combination with the different soil texture inputs?

2. Materials and Methods

2.1. CLM5.0

95 CLM5.0 is a mechanistic land surface model which represents land surface heterogeneity differently from most other land surface models previously used over Africa in continental simulations (Traore et al., 2014; Ghent et al., 2010a ; Weber et al., 2009). While some of the models previously used over Africa had a single layered sub-grid system popularly known as mosaic system, CLM5.0 uses a multi-layered sub-grid hierarchy. This means that in CLM5.0, each grid cell represents multiple land units consisting of vegetated, lake, urban and glacier areas. Each land unit represents multiple columns which could have different soil profiles with autonomously evolving vertical profiles of soil moisture and temperature, and each column has multiple patches of Plant Functional Type (PFT) or Crop Functional Type (CFT) (Lawrence et al., 2018). CLM5.0 therefore has features of great interest for land surface modelling over Africa at a high spatial resolution. Among the numerous improvements of CLM5 compared to its predecessor, are the inclusion of a spatially variable soil depth, replacement of Ball-Berry by Medlyn stomatal conductance and updated irrigation scheduling (Lawrence et al., 2019).

105

The Community Land Model version 5 (CLM5) introduces an advanced structure for modeling soil processes, critical for describing terrestrial hydrology. The total porosity is given by:



110
$$\theta_{\{sat,i\}} = (1 - f_{\{om,i\}}) \cdot \theta_{\{sat,min,i\}} + f_{\{om,i\}} \cdot \theta_{\{sat,om\}} \quad (1)$$

where $f_{\{om,i\}}$ represents organic matter fraction, $\theta_{\{sat,om\}}$ refers to the porosity of the organic matter, $\theta_{\{sat,min,i\}}$ is the porosity of the mineral soil represented as:

115
$$\theta_{\{sat,min,i\}} = 0.489 - 0.00126(\% \text{ sand})_{\{i\}} \quad (2)$$

where $(\% \text{ sand})_{\{i\}}$ is the percentage of sand for the grid cell at level i . To define the relationship between water content in the soil and water potential, the Brooks and Corey model is employed. The exponent B at level i is given by:

120
$$B_i = (1 - f_{\{om,i\}}) \cdot B_{\{min,i\}} + f_{\{om,i\}} \cdot B_{\{om\}} \quad (3)$$

where $B_{\{om\}}$ is the exponent B for the organic matter and

125
$$B_{\{min,i\}} = 2.91 + 0.159 \cdot (\% \text{ clay})_i \quad (4)$$

is for mineral soil where $(\% \text{ clay})_i$ is the percentage of clay for each grid cell i .

Saturated soil matric potential for a grid cell i is given by:

130
$$\Psi_{\{sat,i\}} = (1 - f_{\{om,i\}}) \Psi_{\{sat,min,i\}} + f_{\{om,i\}} \Psi_{\{sat,om\}} \quad (5)$$

where $\Psi_{\{sat,om\}}$ represents saturated organic matter matric potential (mm). The saturated mineral soil matric potential denoted by $\Psi_{\{sat,min,i\}}$ is calculated by:

135
$$\Psi_{\{sat,min,i\}} = -10.0 \times 10^{\{1.88 - 0.0131(\% \text{ sand})_{\{i\}}\}} \quad (6)$$

The mineral soil saturated hydraulic conductivity, $k_{\{sat,min,i\}}$ is calculated based on (Cosby et al., 1984) and expressed as:

140
$$k_{\{sat,min,i\}} = 0.0070556 \times 10^{\{-0.884 + 0.0153(\% \text{ sand})_{\{i\}}\}} \quad (7)$$

while the organic saturated hydraulic conductivity is

145
$$k_{\{sat,om,i\}} = \max\left(0.28 - 0.2799 \times \frac{z_i}{z_{sapric}}, k_{\{sat,min,i\}}\right) \quad (8)$$

where $z_{sapric} = 0.5\text{m}$ as the depth where organic matter assumes the features of sapric peat.



Hydrology in CLM5 involves the representation of water and/or ice at canopy, surface, soil, and aquifer levels. The water balance equation is represented by:

150

$$DS_{c,l} + DS_{c,sn} + DS_{sfc} + DS_{sn} + \sum_{i=1}^{N_{levsoi}} (\theta_{s_{liq,i}} + \theta_{s_{ice,i}}) + DS_{acq} = (q_m + q_{sn} - E_v - E_g - q_{over} - q_{sfcwat} - q_{dr} - q_{rgl} - q_{snsfc})\Delta t \quad (9)$$

155 where $DS_{c,l}$ represents changes in canopy water, $DS_{c,sn}$ changes in canopy snow, DS_{sfc} changes in surface water, DS_{sn} changes in surface snow and DS_{acq} changes in water stored in the aquifer. $\theta_{s_{liq,i}}$ represents changes in soil water, $\theta_{s_{ice,i}}$ represents changes in soil ice at each soil level i . N_{levsoi} refers to the number of soil levels. On the right hand side of the equation, q_m represents rainfall, q_{sn} snowfall, E_v transpiration, E_g evaporation, while q_{over} refers to surface runoff, q_{sfcwat} runoff from surface water storage, q_{dr} drainage, q_{rgl} glacier and lakes runoff and q_{snsfc} snow-capped surface runoff. Δt is the time step. Precipitation ($q_m + q_{sn}$) is intercepted by canopy, which is controlled by leaf area index. The moisture input reaching the surface after evaporative losses from both the 160 vegetation and surface (E_v , E_g) is then divided between surface runoff, surface water storage and infiltration. The units for fluxes are kg/m^2s while storage variables are quantified in kg/m^2 for (Lawrence et al., 2018).

2.2. Soil Texture Information

165 Soil hydraulic and thermal properties are critical for flux and state calculations in LSMs (Zhao et al., 2018). These values are generally obtained from soil texture information through pedotransfer functions, which is also the case for CLM5. Two different soil texture datasets, the IGBP-DIS Soil Dataset and SoilGrids250m dataset, were used as input for CLM5 simulations over Africa, and for the SoilGrids250m dataset three different upscaling methods were compared. The IGBP-DIS soil dataset was generated using the linkage method which is characterized by lack of intra-polygonal variation. This soil texture dataset is the default soil texture information available in 170 CLM5.0. The soil texture dataset provides information for the 10 upper CLM5 soil layers: at 0.0175, 0.0451, 0.0906, 0.1656, 0.2892, 0.493, 0.829, 1.3829, 2.2962 and 3.4332 meter depth. The IGBP-DIS soil dataset provides the number of soil layers, number of map units, and soil texture per map unit layer.

175 ISRIC's SoilGrids250m (Hengl et al., 2017) was produced by machine learning and it is the successor of the SoilGrids1km product (Hengl et al., 2014). Improvements include, e.g., further soil information for deserts and arid areas such as the Sahara desert covering about 30% of Africa's land mass (Tucker & Nicholson, 1999). About 150,000 soil profiles were obtained globally across all continents from both actual and pseudo-observations. Actual observations were from in situ and remote sensing measurements and values reported by national classification systems. Pseudo-observations came from expert assessment of both restricted areas and places with 180 extreme climate conditions like deserts, glaciers, mountain tops, tropical forests, and austere regions. Machine learning approaches which include random forest and logistic regression were applied on 90% of the dataset and a 10-fold cross validation was repetitively performed thereafter using the remaining 10% of the obtained data. SoilGrids250m provides global estimates for soil texture fractions, organic carbon, bulk density, cation exchange capacity, pH and coarse fragments. Compared to SoilGrids1km, SoilGrids250m records in sand, silt and clay 185 contents over 60% relative improvement as explained by the 10-fold cross validation exercise. The Soilgrids250m



unlike the IGBP-DIS was provided at seven standard soil depths of 0, 0.05, 0.15, 0.30, 0.60, 1.00 and 2.00 meters depth.

2.3. Upscaling of Soil Textural properties

Upscaling of soil hydraulic properties is needed when the model grid cell is coarser than the measurement grid cell and downscaling is needed when the model grid cell is finer than the measurement grid cell. SoilGrids250m soil texture information needs to be upscaled to the 3km x 3km resolution of the CLM5 model for Africa. One CLM5 grid cell contains therefore 144 SoilGrids250m grid cells. Three upscaling methods of soil texture information were compared in this work:

- 195 (i) Simple averaging of the soil texture values for all the SoilGrids grid cells which are contained in a larger CLM grid cell (e.g., Kochendorfer and Ramírez, 2010).
- (ii) Selection of the dominant soil type (according to USDA soil classification) in a CLM grid cell and use of the soil texture values for that soil type for the complete CLM grid cell. This method was for example used in Tafasca et al. (2019). The dominant soil type is any soil type with the highest representation among the 144 SoilGrids grid cells.
- 200 (iii) Random selection of a single SoilGrid cell and use of the soil texture values for this grid cell for the complete 3km x 3km CLM model grid cell. This method was motivated due to its ability to avoid spatial averaging or smoothing. Although it introduces larger local biases in the soil input parameters and therefore also model output variables, over larger areas it is expected not to induce systematic biases, as local biases for some grid cells will be cancelled out by local biases for other grid cells in
205 the other direction. In addition, as soil texture is not averaged or smoothed before processing it through the non-linear simulation model, it is expected that also model output variables, averaged over larger areas, are unbiased.

2.4. Meteorological Forcings

210 In this work, the impact of three different meteorologic forcing datasets with different temporal resolution, in combination with the different soil texture input datasets, was investigated:

- 215 (i) **CRUNCEPv7**. CRUNCEPv7 dataset is a combination of CRU (Climate Research unit Time Series) 3.24 (Harris, 2013) and National Centre for Environmental Protection (NCEP) reanalysis (Kalnay et al., 1996). The data are available for the period between 1901 and 2016 with a horizontal resolution of 0.5° and 6 hourly temporal resolution. Precipitation, cloudiness, temperature, and relative humidity were taken from CRU while wind speed, pressure and long wave radiation were obtained from NCEP. Since both GSWP3 and CRUNCEPv7 datasets were provided for use in CLM by the developers there is no additional processing needed to use these datasets in CLM5.
- 220 (ii) **GSWP3**. The Global Soil Wetness Project version 3 dataset is a 3-hourly, 0.5° horizontal resolution atmospheric forcing product. The data are available for the period between 1900 and 2014 and are based on NCEP's 20th century reanalysis project (Compo et al., 2011). Though the 20th century



project dataset was published at 2° horizontal resolution, the GSWP version 3 dataset was
 downscaled to 0.5° horizontal resolution using a spectral nudging technique (Yoshimura and
 Kanamitsu, 2008). Four out of seven variables namely air temperature, precipitation, long and short
 wave radiation were bias corrected using Climate Research Unit’s CRU Tsv3.21 (Harris, 2013),
 Global Precipitation Climatology Centre’s GPCCv7 (Schneider et al., 2014) and surface radiation
 budget datasets (Lawrence et al., 2019). GSWP3 is the default forcing provided with the CLM5
 Model (Lawrence et al., 2018).

(iii) **WFDE5.** The WFDE5 dataset was created by using the WATer and global CHange (WATCH)
 Forcing Data methodology to process near surface 5th generation ECMWF (European Centre for
 Medium-range Weather Forecasts) ReAnalysis (ERA5) variables. WFDE5 was provided globally
 on a regular lonlat grid at 0.5° x 0.5° spatial resolution at hourly time steps. It has therefore the
 highest temporal resolution of the considered atmospheric forcing datasets in this study. WFDE5
 correlates better with FLUXNET2015 datasets at each site than WFDEI (Traore et al. 2014).
 Another advantage WFDE5 has over the higher spatial resolution ERA5 data set is that the monthly
 precipitation totals were bias corrected using precipitation data from the Climate Research unit Time
 Series (CRU TS) and Global Precipitation Climatology Centre (GPCC). This is important as
 precipitation has a large impact on LSM simulations compared to other meteorological forcings
 (Bucchignani et al., 2016) over Africa. Table 1 summarizes details regarding the different
 meteorological forcing datasets used in this work.

Table 1. Main properties of the reanalysis datasets CRUNCEPv7, GSWPv3 and WFDE5 used as
 inputs for simulations with CLM5.0.

Properties	CRUNCEPv7	GSWP3	WFDE5
Spatial resolution	0.5°	0.5°	0.5°
Temporal resolution	6 Hourly	3 Hourly	1 Hourly
Longitudinal extent	0 to 360° East	0 to 360° East	-180°W to 180°E

2.5. Model Setup

CLM5.0 was run in this work in land only mode, i.e., instead of coupling CLM5 with an atmospheric model,
 atmospheric reanalysis datasets are used as external forcings to the land surface model. Atmospheric input to CLM
 includes precipitation, incoming shortwave radiation, air temperature, surface air pressure, specific humidity,
 wind speed and incoming longwave radiation and is available for CRUNCEP every 6 hours, GSWP every 3 hours
 and for WFDE5 hourly. But since model time step is 30 minutes, precipitation is divided equally over the different
 model time steps. For air temperature, surface air pressure, specific humidity and wind speed, all values are
 interpolated to model time steps using nearest neighbour algorithm. For solar radiation, cosine of the solar zenith



angle is used to ensure a smoother diurnal cycle, while preserving the total radiation from the atmospheric input data.

255 Sixteen plant functional types were activated, and transient CO₂ and aerosol deposition rates. All twelve model simulations (Table 2) apply monthly leaf area index (LAI) as observed from satellite phenology. A spatially varying soil thickness dataset with values ranging from 0.4 m to 8.5 m was applied (Pelletier et al., 2016). The land cover description is based on 1km resolution Moderate Resolution Imaging Spectroradiometer (MODIS) products. Land Cover Type is from MCD12Q1 version 5 which provides annual land cover intervals between
260 2000 and 2015.

Simulations were performed over the CORDEX Africa domain which covers longitude -24.64°W to 60.28°E and latitude 45.76°S to 42.24°N (results over African continent only). The horizontal resolution for all model simulations was approximately 0.027°, i.e. about 3 km. This discretization results in 10,033,920 grid cells.

265 Simulations period was from the 1st of January 2012 to the 31st of December 2014 and results for the first year were discarded (spin up year). Although the model time step size was 30 minutes, most results are presented as monthly sums (at regional and local scales). For continental scale results, yearly sum of evapotranspiration (ET), surface runoff, and subsurface runoff were computed as well as seasonal mean soil moisture contents.

270 To validate the role of soil texture input to CLM5.0 in combination with the temporal resolution of the atmospheric forcings, the hourly WFDE5 forcings were also aggregated to 3 hours and used in new simulations. This was done to reveal differences between the simulation outcomes of WFDE5 at hourly and 3 hourly temporal resolution. The results were analysed at monthly resolution as well for regional and local time series.

275 A metric termed “average margin” was introduced to quantify the impact of temporal resolution of atmospheric forcings in combination with soil texture map variation. The four (4) soil texture maps were considered each providing a unique output at every timestep within the time series. A simulated variable for a certain atmospheric forcings- soil texture map combination at a given time step is denoted by $M_1(t)$, $M_2(t)$, $M_3(t)$ and $M_4(t)$. The difference in the maximum and minimum simulated value for the variable, between the soil texture maps at a given time step is then computed as:

$$280 \quad D(t) = \max(M_1(t), M_2(t), M_3(t), M_4(t)) - \min(M_1(t), M_2(t), M_3(t), M_4(t)) \quad (10)$$

and the average margin is given by:

$$A = \frac{1}{T} \sum_{t=1}^T D(t) \quad (11)$$

where T represents the total number of time steps in the time series.

285 Table 2: Summary of CLM5 experiments in this study, combining different soil texture input information and atmospheric forcings.

Experiment	Soil Texture	Forcing
FAO_CRU	FAO	CRUNCEP



SGd_CRU	SoilGrids-Dominant	CRUNCEP
SGm_CRU	SoilGrids-Mean	CRUNCEP
SGr_CRU	SoilGrids-Random	CRUNCEP
FAO_GSW	FAO	GSWP
SGd_GSW	SoilGrids-Dominant	GSWP
SGm_GSW	SoilGrids-Mean	GSWP
SGr_GSW	SoilGrids-Random	GSWP
FAO_WFD	FAO	WFDE5
SGd_WFD	SoilGrids-Dominant	WFDE5
SGm_WFD	SoilGrids-Mean	WFDE5
SGr_WFD	SoilGrids-Random	WFDE5

3. Results and Discussion

3.1. Continental Results

290 3.1.1 Evaporation

Figure 1 shows actual ET estimates over Africa for the different soil texture maps used in this study and the different atmospheric forcings. Continental average ET and local ET maxima were estimated for all 12 simulations for the reference period of 2013-2014.

295 The soil texture map has in general only a limited impact on simulated ET. For CRUNCEP forced simulations the yearly ET varies among the soil maps between 452.9 mm/year and 454.4 mm/year, with the lowest ET for the FAO soil texture map and slightly higher ET for the SoilGrids texture maps. Also, for GSWP forced simulations we find the lowest simulated ET for the FAO soil texture map (438.7 mm/year), while the highest simulated ET is only marginally higher (439.6 mm/year). Simulated ET is highest for the SoilGrids soil map which is randomly upscaled. Also, for the WFDE5 simulations differences in simulated ET are very small and vary between 442.5
 300 mm/year (FAO) and 443.5 mm/year (SoilGrids, randomly upscaled). These numbers also illustrate that the impact of variations in soil texture input are much smaller than variations in atmospheric forcings. While the four different soil texture maps result in maximum variations in average yearly ET over the African continent of only ~1mm for a given atmospheric forcing, the variations in atmospheric forcings result in maximum variations in average yearly ET over the African continent around 14mm/year, for a given soil texture dataset. Specifically, the upscaling
 305 procedure of the soil texture information exhibits negligible effects on the mean annual estimates of evapotranspiration over Africa. Also, the maximum simulated ET for a grid cell over Africa is hardly affected by the soil texture map input (<1mm/year), with even smaller variations among soil texture maps than the continental



average. On the other hand, variations in atmospheric forcings affect the local maximum simulated yearly ET stronger with variations among forcings ~36mm/year.

310

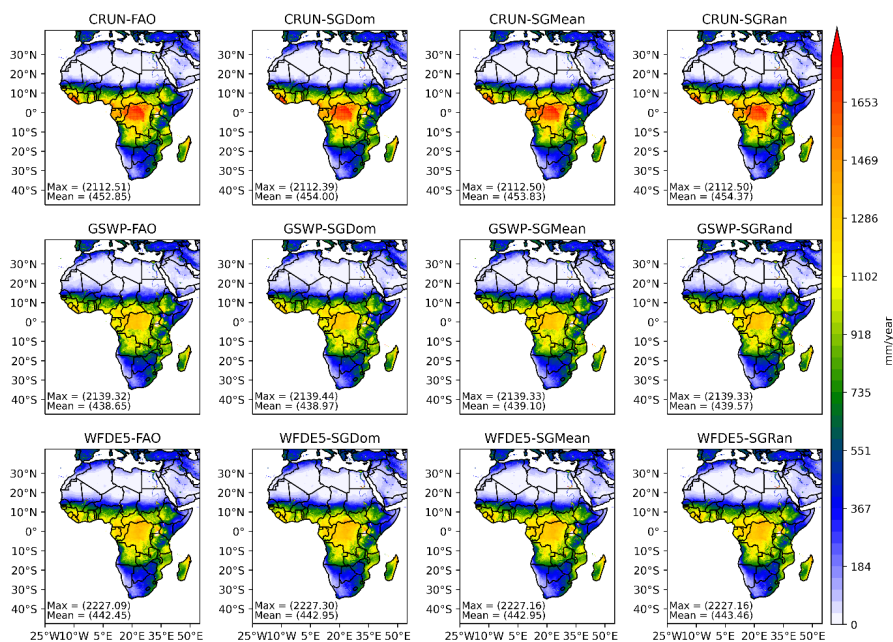


Figure 1: Spatial distribution of simulated mean annual evapotranspiration over Africa. Upper row: CRUNCEP forced simulations with, from left to right, FAO, Dominant, Mean and Random upscaled soil texture map inputs. Middle row: like row 1, but GSWP forced simulations. Bottom row: similar to row 1, but WFDE5 forced simulations.

315

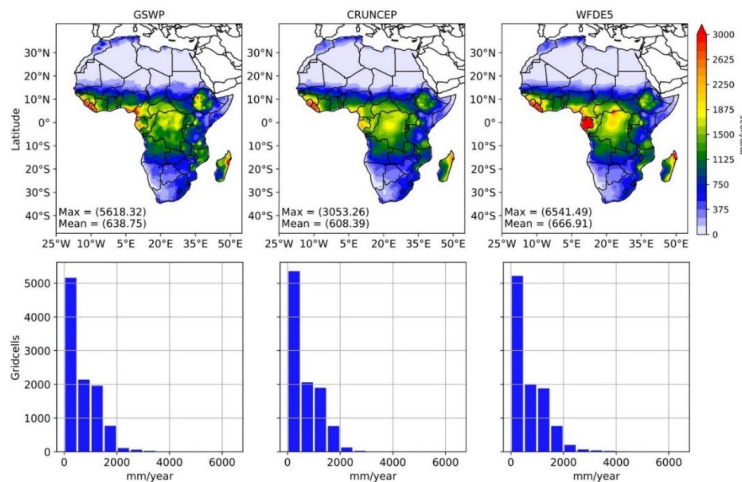




Figure 2: Mean annual rainfall (2013-2014) distribution of CRUNCEP, GSWP and WFDE5 datasets over Africa. Row 1: spatial representation. Row 2: rainfall distribution into bins of 500mm/year.

320

3.1.2 Surface runoff

Also, the surface runoff is not strongly affected by variations in the soil texture map. For all three atmospheric forcings, the average surface runoff over the African continent is almost the same for the four different soil texture maps and differences in surface runoff are never larger than 0.3mm/year, for a given atmospheric forcing. When
325 examining the influence of soil texture maps on surface runoff, it becomes evident that the disparities between the various SoilGrids maps, generated using different upscaling methods, are minimal. The maximum difference in continental averages of surface runoff between the SoilGrids soil texture maps with the highest and lowest values is only 0.01-0.02 mm/year, depending on the atmospheric forcing. However, slightly larger differences are observed when comparing the FAO soil texture map with the SoilGrids texture maps, with a maximum variation
330 of 0.20-0.26 mm/year, again depending on the atmospheric forcing. These findings indicate that while the upscaling process of soil texture maps does not significantly impact simulated surface runoff with CLM5, the source and type of soil texture maps employed do have a small, yet perceivable, influence on the results.

On the other hand, the atmospheric forcing shows a much larger impact on average surface runoff over Africa with approximately 94 mm/year for CRUNCEP (6 hourly temporal resolution), 114 mm/year for GSWP (3-hourly
335 temporal resolution of atmospheric forcings) and 122 mm/year for WFDE5 (hourly forcings). Spatial details can be found in Figure 3. The substantial difference of 28 mm/year in average annual surface runoff between WFDE5 and CRUNCEP helps explain why ET estimates are higher for CRUNCEP by 11 mm/year. The increased surface runoff in the WFDE5 forced simulations reduces the availability of water for ET processes.

The differences in surface runoff could be related to the temporal resolution of the atmospheric forcings. A higher
340 temporal resolution of the atmospheric forcings as for WFDE5 will result in higher peaks of precipitation intensity, whereas a coarser temporal resolution of 6 hours like for CRUNCEP will average out intensive precipitation over longer time periods with less high peaks in precipitation intensity. As surface runoff is generated under conditions of (very) high precipitation intensity, it can be expected that the temporal resolution of the atmospheric forcings will affect the simulated amount of surface runoff.

345

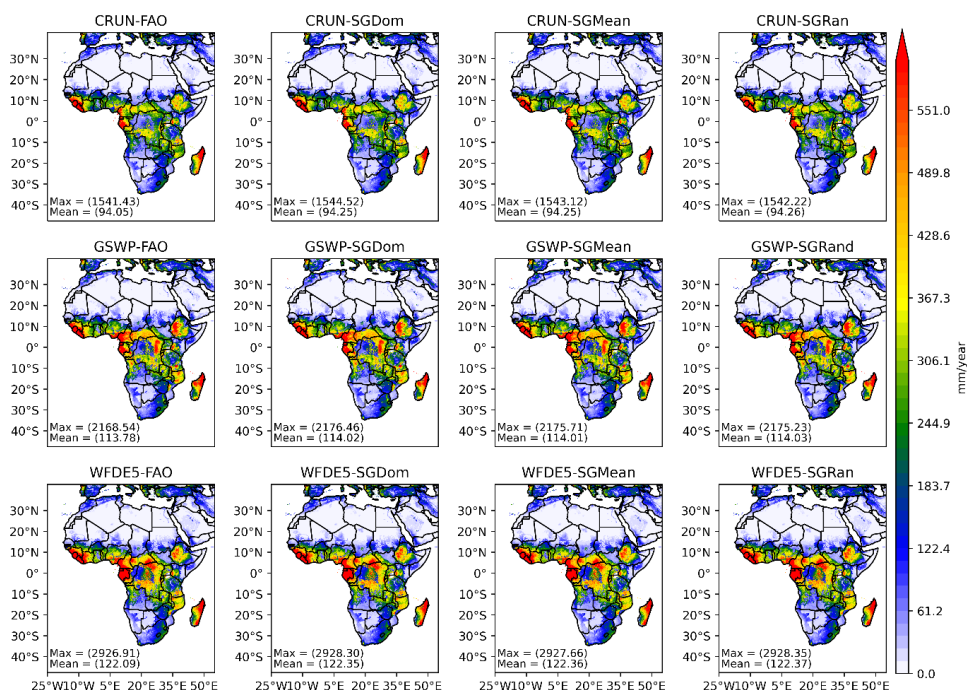


Figure 3: Spatial distribution of simulated mean annual surface runoff over Africa. Upper row: CRUNCEP forced simulations with, from left to right, FAO, Dominant, Mean and Random upscaled soil texture map inputs. Middle row: similar to row 1, but GSWP forced simulations. Bottom row: similar to row 1, but WFDE5 forced simulations.

350

3.1.3 Subsurface runoff

Simulated subsurface runoff across the African continent is in general low in most regions and across all simulation scenarios, typically below 250 mm/year. The estimation of subsurface runoff is more significantly influenced by soil texture variations and the upscaling of soil texture properties compared to ET and surface runoff simulations. The most substantial differences in simulated subsurface runoff are observed between the FAO soil map and the SoilGrids250m maps, while the disparities among the upscaled SoilGrids250m maps are smaller. For CRUNCEP forcings, the difference between the maximum and minimum simulated subsurface runoff among the soil texture maps (averaged over Africa) is 11.3 mm/year, whereas it is 2.1 mm/year among the upscaled SoilGrids maps. For GSWP, these differences are 11.6 mm/year and 2.4 mm/year, respectively, while for WFDE5, they are 26.0 mm/year and 14.5 mm/year, respectively. Notably, for WFDE5 (with 1-hourly forcings), the differences in simulated subsurface runoff among the different upscaled SoilGrids maps are considerably larger than for the other forcings. The variations in maximum subsurface runoff values among soil texture maps are more pronounced than for the mean subsurface runoff, particularly for CRUNCEP and WFDE5, where the differences among upscaled SoilGrids maps are also substantial. Refer to Figure 4 for more detailed information and numerical values.

365



On the other hand, the spatially averaged subsurface runoff over Africa showed considerable variations among atmospheric forcings: 17-29 mm/year for CRUNCEP, between 36 and 48 mm/year for GSWP and 42-68 mm/year for WFDE5. Like surface runoff patterns, WFDE5 has the highest values, followed by GSWP, while CRUNCEP simulations yield the lowest subsurface runoff estimates. This discrepancy can be attributed to the higher average precipitation in WFDE5 over Africa (refer to Figure 2). However, despite the higher precipitation, WFDE5 does not yield higher ET than CRUNCEP (the average ET is 11 mm/year smaller across the continent). Instead, the higher precipitation leads to increased surface runoff and subsurface runoff. The simulation results for GSWP fall in between those of WFDE5 and CRUNCEP.

In summary, for subsurface runoff simulation, both variations in atmospheric forcings and soil texture, including different upscaling methods, play an important role.

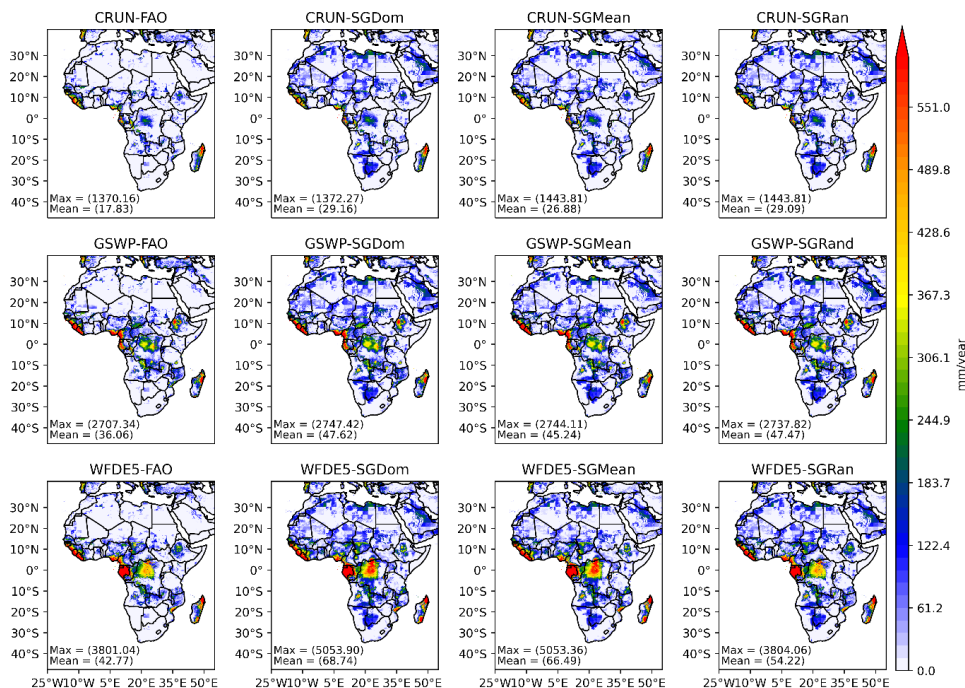


Figure 4: Spatial distribution of simulated mean annual sub-surface runoff over Africa. Upper row: CRUNCEP forced simulations with, from left to right, FAO, Dominant, Mean and Random upscaled soil texture map inputs. Middle row: like row 1, but GSWP forced simulations. Bottom row: like row 1, but WFDE5 forced simulations.

380

3.1.4 Soil moisture

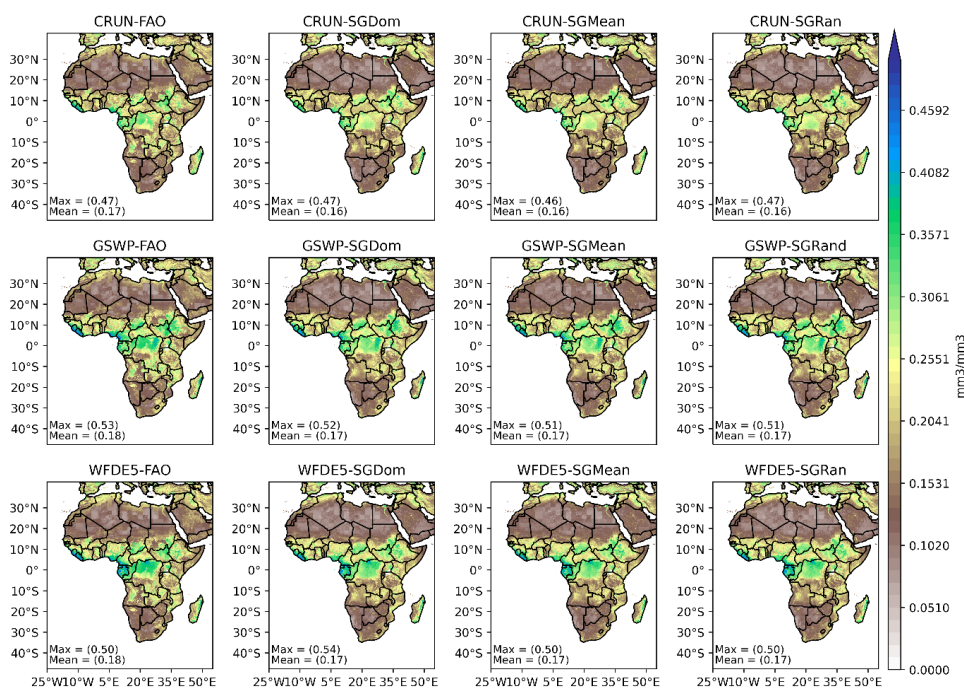
Soil moisture estimates were obtained by calculating the weighted average of soil moisture over the top 2 meters of the soil profile in CLM5. Mean annual maxima and averages have also been analysed for each season, as seasonal analysis of soil moisture reflects seasonal changes in hydrological processes (Myeni et al., 2019), and allows a better understanding of the relationship between vegetation and water availability (Huber et al., 2011). Specifically, for the boreal summer season (JJA), the average simulated soil moisture across the African continent

385



varies between 0.02 cm³/cm³ in the Sahara and 0.54 cm³/cm³ in both Equatorial Guinea and the coasts of Sierra Leone among the 12 simulations (Figure 5). The upscaled soil texture maps give all very similar continental averages of soil moisture for the summer season. The source of the soil texture maps (FAO vs SoilGrids) resulted in some variation in the continental soil moisture averages. This suggests that the source of a soil texture map could influence soil moisture estimates by a land surface model more than the upscaling procedure of the soil texture information. The WFDE5 atmospheric forcings are associated with more variation in simulated soil moisture among the 4 soil texture maps than the other atmospheric forcings.

Like for ET and surface runoff, varying the atmospheric forcing impacted soil moisture more than variations in soil texture input. CRUNCEP forced simulations (6 hourly timesteps) gave lower maximum soil moisture values (0.46-0.47 cm³/cm³) than GSWP (3 hourly timesteps; 0.51-0.53 cm³/cm³) and WFDE5 (hourly timesteps; 0.50-0.54 cm³/cm³) forced simulations. This difference is likely attributed to lower precipitation amounts in the CRUNCEP forced simulations, combined with slightly higher ET values in comparison to simulations with the other forcings.



400 **Figure 5: Spatial distribution of simulated soil water content in the JJA season over Africa. Top row: CRUNCEP forced simulations with FAO, Dominant, Mean and Random upscaled soil texture map inputs. Middle row: like top row, but GSWP forced simulations. Bottom row: like top row, but WFDE5 forced simulations.**

405 3.2 Regional Results

Iturbide et al. (2020) updated the IPCC climate reference regions for subcontinental analysis based on, amongst others, coherence of climate variables. The new reference regions for Africa include the Mediterranean, Sahara,



West Africa, North-East Africa, Central Africa, Central-East Africa, South-West Africa, and South-East Africa. Here we combined South-East Africa and Madagascar into one region. Figure 6 shows the African sub-regions. 410 The eight regions are used as basis to calculate region-specific water balance components. Two regions are discussed while more information for other regions is available as supplementary material. Water balance components are also calculated as monthly sums and shown in a time series.

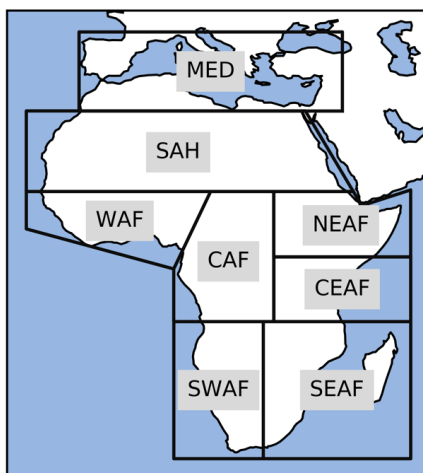
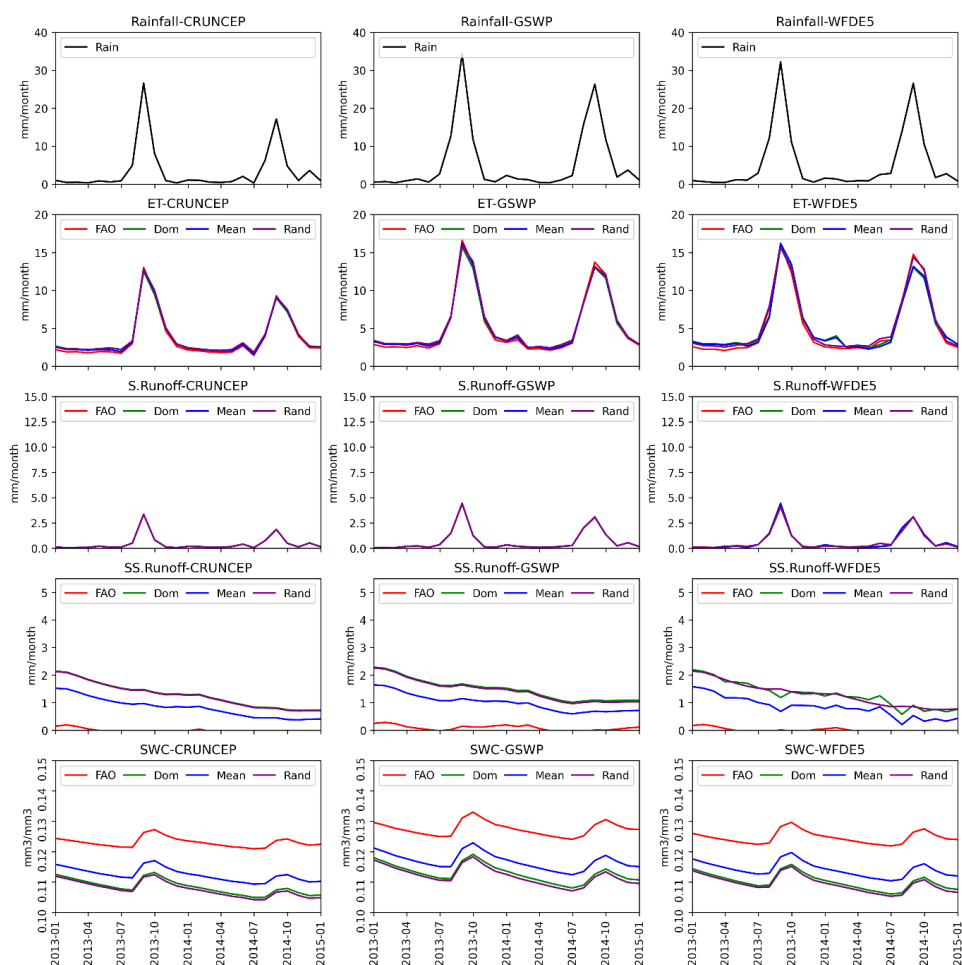


Figure 6: Modified classification of Africa into climate regions according to Iturbide et al. (2020).

415

3.2.1 Sahara region

The Sahara region is the most moisture deficient region in Africa with rainfall less than 40mm/month for the entire simulation period (see Figure 7, row 1). Rainfall over the region was highest in August 2013 (around 30mm/month) and was near 0mm/month for many other months, especially in the winter season.



420

Figure 7: Monthly regional mean of water balance components over the Sahara. Rows 1-5 show precipitation, actual ET, surface runoff, subsurface runoff, and soil water content respectively. Left, middle and right columns show the same variables for CRUNCEP, GSWP and WFDE5 atmospheric forcings respectively. The lines in the figures represent results for different soil textures as input. Red line: FAO, green line: SoilGrids-Dominant, blue line: SoilGrids-Mean and purple line: SoilGrids-Random.

425

Also at the regional scale, for the example of the Sahara region, simulated evapotranspiration and surface runoff differed little among different soil texture maps. The average margin in actual ET among soil texture maps is only 0.4mm/month for both CRUNCEP and GSWP forcings, and 0.8mm/month for WFDE5 forcing. Evapotranspiration (ET) simulated by the CLM5 model varied more as function of the atmospheric forcing and can for a given soil texture map vary up to a few mm per month between different atmospheric forcings.

430

Simulated surface runoff exhibits similar patterns for all soil texture maps, with minimal surface runoff and slight increases during months with higher precipitation. The average monthly differences in surface runoff between the different soil texture maps are smaller than 0.1mm/month. Subsurface runoff shows a decreasing trend, which is

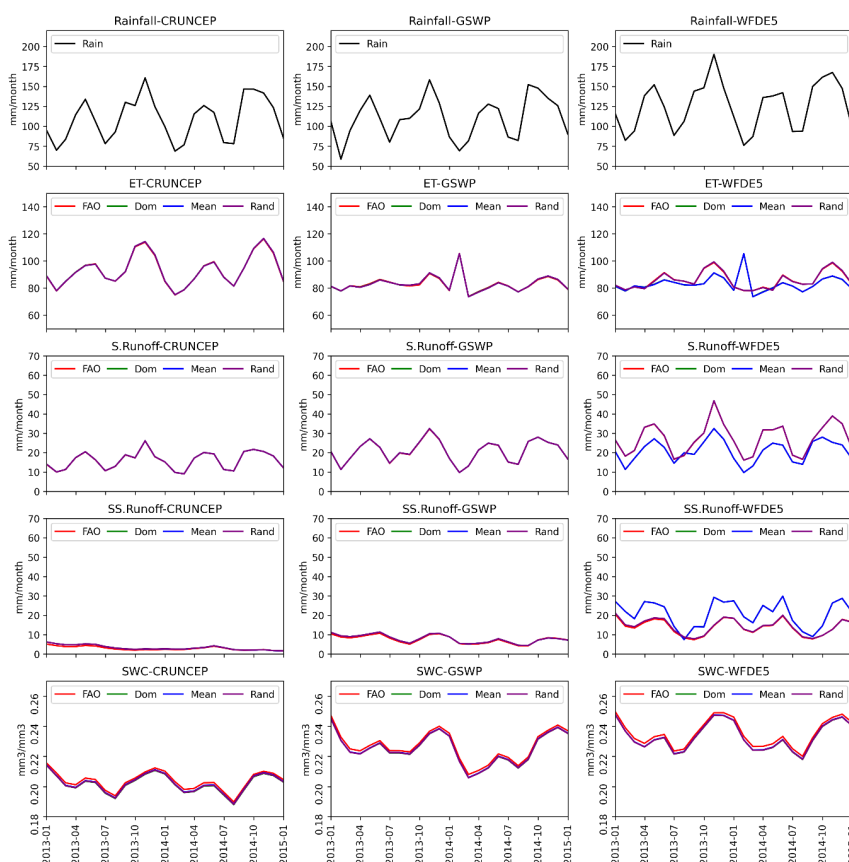


435 attributed to initially higher groundwater levels. While subsurface runoff is generally small in absolute terms, the
different soil texture maps result in varying relative amounts of subsurface runoff. Simulated average soil moisture
content over the Sahara region is consistently low, with values around 0.12 cm³/cm³. These values, which are not
extremely low in spite of very limited precipitation, could be attributed to the amount of loamy soil over the region
(Figure S1) with higher residual soil moisture than in sandy soils. Differences in simulated soil moisture among
440 the soil texture maps are primarily influenced by the variations in soil properties used in each map.

The different soil texture inputs to the WFDE5 forced simulations result in larger differences in simulated ET and
surface runoff compared to the other atmospheric forcings, for regions with low soil moisture content like the
Mediterranean (Figure S6) and South-West Africa (Figure S10). The higher temporal resolution (1 hour) of the
WFDE5 atmospheric forcing leads to varying surface runoff compared to forcings with lower temporal resolutions
445 (3-hour or 6-hour). Additionally, the higher temporal resolution of other variables in the atmospheric forcings,
such as global radiation (Figure S19), also affects the simulation of evapotranspiration.

Overall, these findings over the Sahara and other low moisture regions like the Mediterranean and South-West
Africa highlight the influence of atmospheric forcing and its temporal resolution, soil texture maps variation, and
their interactions on the simulation of ET, surface runoff, subsurface runoff, and soil moisture content across
450 different regions of Africa.

3.2.2 Central Africa



455 **Figure 8: Monthly regional mean of water balance components over Central Africa. Rows 1-5 show precipitation, actual ET, surface runoff, subsurface runoff and soil water content respectively. Left, middle and right columns show the same variables for CRUNCEP, GSWP and WFDE5 atmospheric forcings respectively. The lines in the figures represent results for different soil textures as input. Red line: FAO, green line: SoilGrids-Dominant, blue line: SoilGrids-Mean and purple line: SoilGrids-Random.**

460 Central Africa encompasses the Congo rainforest, the second-largest rainforest in the world, consisting of evergreen and semi-evergreen deciduous forests (Aloysius & Saiers, 2017) and stands out as one of the most moisture-rich regions in Africa, characterized by a regional mean rainfall ranging from 50 to 200mm/month. The proximity to the equator results in frequent rainfall events due to recurrent convective precipitation events. The dense vegetation in Central Africa contributes to high transpiration rates, which are supported by the substantial amounts of rainfall.

465 Once again, we observe that only the WFDE5 atmospheric forcings exhibit variations in average ET values across different soil texture maps, as shown in Figure 8. On average (over the years 2013 and 2014), the soil texture maps with the highest and lowest monthly averaged ET differ by 0.5mm/month for CRUNCEP and GSWP, but by 5.8mm/month for WFDE5. The monthly averaged surface runoff values for CRUNCEP and GSWP show little



470 variation among different soil texture maps. However, for WFDE5, the SoilGrids map upscaled with random
selection results on average in a 6.7mm/month higher surface runoff than the other soil texture maps. Regarding
subsurface runoff, GSWP and CRUNCEP simulations exhibit, at most, a 0.4mm/month difference in average
monthly subsurface runoff among different soil texture maps, whereas WFDE5 shows a difference of
7.0mm/month. The soil moisture maps display very similar average values across all atmospheric forcings and
soil texture maps.

475 Other moisture rich regions including West Africa (Figure S7), North-East Africa (Figure S8), Central-East Africa
(Figure S9) and South-East Africa (Figure S11) also show that WFDE5 forced simulations resulted in clear
differences in simulated ET, surface runoff and subsurface runoff for the different soil texture inputs. On the other
hand, soil moisture did not show clear differences for the different soil texture maps.

3.3. Local Results

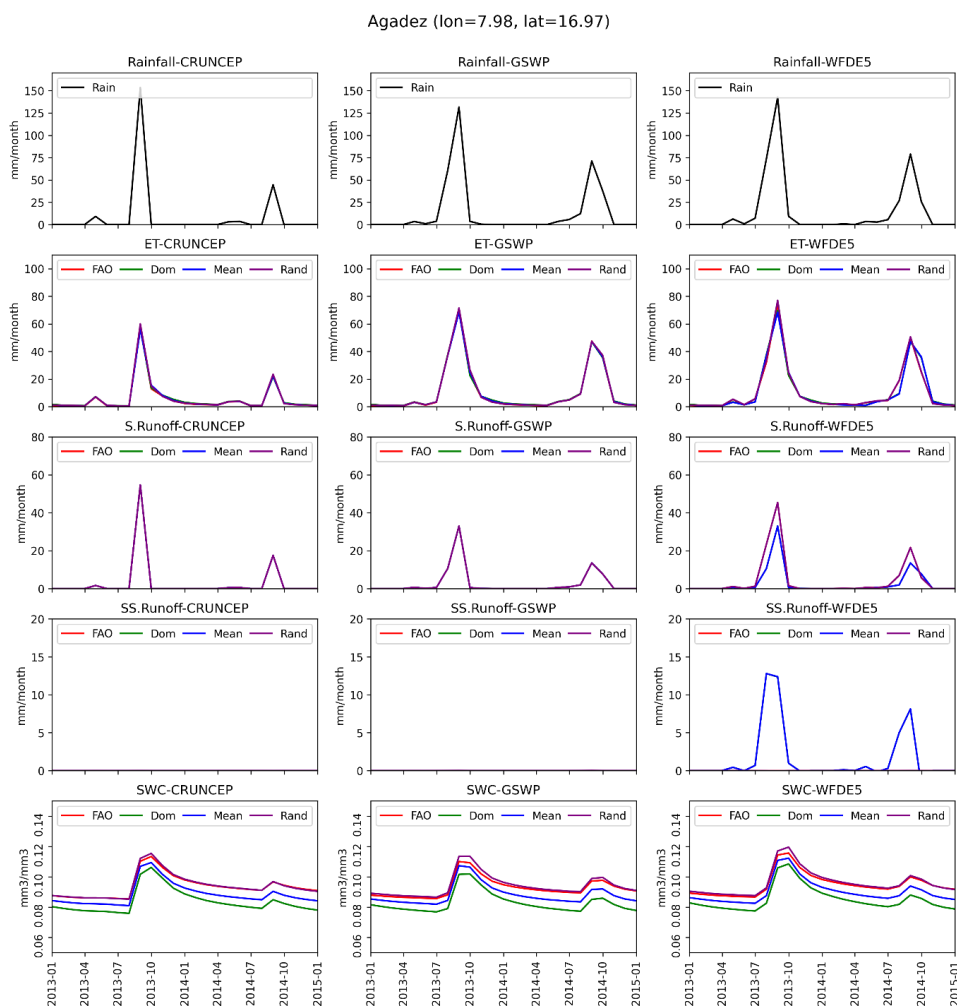
480 We now look at the results at the local scale (grid scale) to analyze further the impact of the variation of soil
texture maps and atmospheric forcings on simulation outcomes. We selected one location for each of the eight
climate regions: Cairo (Egypt, Mediterranean), Agadez (Niger, Sahara), Abuja (Nigeria, West Africa), Addis-
Ababa (Ethiopia, North-East Africa), Salong (DR Congo, Central Africa), Daar-es-Salaam (Tanzania, Central-
East Africa), Windhoek (Namibia, South-West Africa) and Maseru (Lesotho, South-East Africa).

485 3.3.1 Agadez

Agadez, situated at 16.97°N and 7.98°E, experienced its highest precipitation of 126mm in August 2013 and
received no rainfall during several winter months. The results for Agadez indicate a close association between ET
peaks and precipitation peaks, as ET in this region, including the Sahara, is limited by water availability. Despite
a five-month period without rainfall from September 2013 to January 2014, ET values in Agadez remained
490 nonzero (1.5mm/month) between January 2014 and April 2014. This can be attributed to irrigation practices
automatically applied to sustain irrigated crops when the soil moisture content falls below a critical threshold
within CLM5.

The WFDE5 forced simulations for Agadez (Figure 9) show that different (upscaled) soil texture maps yield
varying monthly ET, surface runoff, and subsurface runoff values. On average (over the years 2013 and 2014),
495 the soil texture maps with the highest and lowest monthly averaged ET differ by 0.7mm/month for CRUNCEP,
0.9mm/month for GSWP, and 1.8mm/month for WFDE5 which correspond to 7%, 8% and 12% of monthly
average evapotranspiration respectively. This can be attributed to low rainfall. Model simulations driven by
CRUNCEP or GSWP show no variation in surface runoff as function of the soil texture map, while slight
variations in surface runoff are found for WFDE5. A similar pattern is observed for subsurface runoff. Regarding
500 soil moisture, small but systematic differences between soil texture maps are discernible.

Overall, the results for Agadez demonstrate the influence of soil texture map variation on ET, surface runoff and
subsurface runoff, with WFDE5 simulations exhibiting more pronounced variations compared to CRUNCEP and
GSWP forcings. These findings underscore the importance of soil texture representation and temporal resolution
of the atmospheric forcing in capturing the hydrological processes in Agadez and similar locations.



510 **Figure 9: Local monthly mean of water balance components over Agadez. Rows 1-5 show precipitation, actual ET, surface runoff, subsurface runoff and soil water content respectively. Left, middle and right columns show the same variables for CRUNCEP, GSWP and WFDE5 atmospheric forcings respectively. The lines in the figures represent results for different soil textures as input. Red line: FAO, green line: SoilGrids-Dominant, blue line: SoilGrids-Mean and purple line: SoilGrids-Random.**

3.3.2 Abuja

515 Abuja, situated in Nigeria at coordinates 9.07°N, 7.30°E, exhibits a distinct yearly precipitation cycle characterized by high rainfall during the summer months, with precipitation exceeding 200mm/month. Conversely, the winter season is dry, with months devoid of any rainfall (Figure 10). ET peaks in Abuja typically occur approximately one month or more after the peak of rainfall, as observed in 2014.

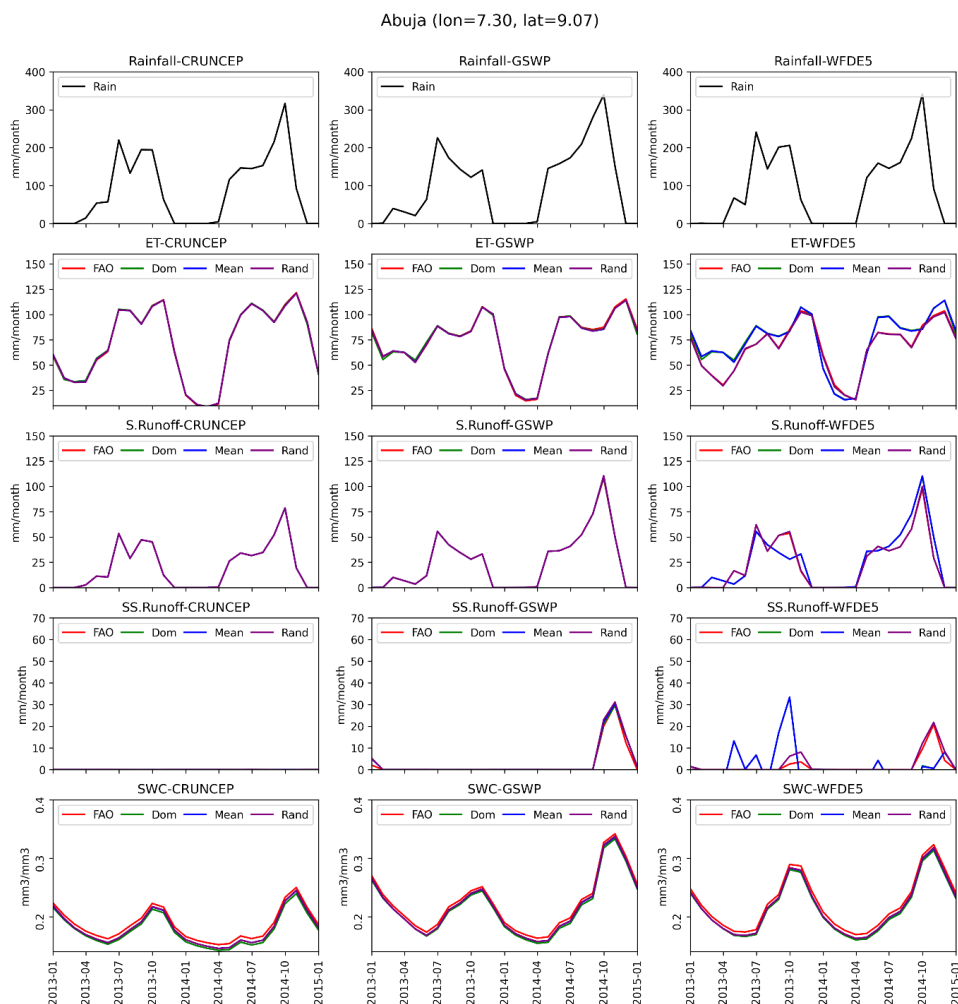


520 Simulated ET, surface runoff, and subsurface runoff in Abuja demonstrate variations across different soil texture maps, particularly noticeable with the high temporal resolution atmospheric forcings provided by WFDE5. Subsequently, we calculated the average of these maximum differences over the years 2013 and 2014. In terms of ET, WFDE5 displays the largest average differences between soil texture maps (10.4mm/month), followed by GSWP (1.4mm/month) and CRUNCEP (1.0mm/month). Regarding surface runoff, WFDE5 also yields the largest difference (7.5mm/month), while CRUNCEP and GSWP exhibit negligible differences (<0.2mm/month).

525 Similarly, the ranking of differences in subsurface runoff follows the same pattern, with WFDE5 showing the largest disparities (7.7mm/month), followed by GSWP (0.4mm/month), and finally CRUNCEP (0.0mm/month). Notably, the FAO soil texture map consistently results in slightly higher soil water content (SWC) compared to the SoilGrids soil texture maps for all atmospheric forcings (as depicted in the lower row of Figure 12). However, these differences in SWC do not exceed 0.01cm³/cm³ across all atmospheric forcings.

530 Similar patterns are observed for other locations, including Cairo (Figure S12), Addis-Ababa (Figure S14), Salong (Figure S15), Daar-es-Salaam (Figure S16), Windhoek (Figure S17), and Maseru (Figure S18). WFDE5 forced simulations exhibit larger variations in simulated ET, surface runoff, and subsurface runoff among different soil texture maps compared to the other atmospheric forcings. Simulated soil moisture content shows minimal variations among the different soil texture maps for a given atmospheric forcing.

535



540 **Figure 10: Local monthly mean of water balance components over Abuja. Rows 1-5 show precipitation, actual ET, surface runoff, subsurface runoff and soil water content respectively. Left, middle and right columns show the same variables for CRUNCEP, GSWP and WFDE5 atmospheric forcings respectively. The lines in the figures represent results for different soil textures as input. Red line: FAO, green line: Soilgrids-Dominant, blue line: SoilGrids-Mean and purple line: SoilGrids-Random.**

3.4. Discussion

545 The simulation results over Africa suggest that the atmospheric forcings exert an important control on the ET estimates, while soil texture is important for simulating surface and subsurface runoff. The simulation results also suggest that the temporal resolution of atmospheric forcings could influence the simulation outcomes clearly, especially surface and subsurface runoff, and the interaction with soil texture seems to play a role here.

The analysis of water budget components shows differences in simulated ET, surface runoff and subsurface runoff for the different upscaled soil texture maps in combination with WFDE5 forced simulations, but not in combination with other atmospheric forcings. We observed for ET and surface runoff across all regions, that

550



555 higher temporal resolution led to higher differences in ET and surface runoff between soil texture map outcomes with the largest differences for WFDE5 (hourly resolution), followed by GSWP (3 hourly resolution) and CRUNCEP (6 hourly resolution). For subsurface runoff, higher temporal resolution did not result in such a systematic pattern in moisture-rich regions with rainfall above 200mm/month. However, in moisture deficient regions with precipitation less than 150mm/month higher temporal resolution of atmospheric forcing is associated with more variation in subsurface runoff for different soil texture maps. The temporal resolution of the atmospheric forcings did not result in different soil moisture results for each soil texture map, but in all regions it was observed that the FAO soil texture map resulted in different soil moisture than the Soilgrids250m soil texture maps partially confirming the findings of Tafasca et al. (2019) which showed that soil mapping had a stronger influence on soil moisture compared to fluxes.

To further validate the role of the temporal resolution of atmospheric forcings, WFDE5 forcings were aggregated (from hourly data) so that they varied only on a 3 hourly basis, like GSWP and simulations were performed to examine the impact on ET, surface runoff, subsurface runoff and soil moisture content both regionally and locally. We compare now 3H-WFDE5 (3 hourly), GSWP (3 hourly) and WFDE5 (1 hourly).

565

Table 3: Difference in simulated variables between soil texture maps for GSWP atmospheric forcings (3 hourly), WFDE5 atmospheric forcings (3 hourly) and WFDE5 atmospheric forcings aggregated to hourly resolution over West Africa (mm/month).

Variable	3H-WFDE5	GSWP	WFDE5
Evapotranspiration	0.61	0.60	4.34
Surface Runoff	0.09	0.07	2.68
Subsurface Runoff	0.59	0.48	3.00
Soil Moisture	0.00	0.00	0.00

570 Table 3 shows the impact of varying soil texture map inputs on different water balance component for West Africa. Simulated variables show much less variation as function of soil texture map input for 3-hourly aggregated WFDE5 forcings and GSWP (3 hourly) compared to 1-hourly WFDE5 forcings. Similar results are found for Abuja (Table 4), where 3H-WFDE5 and GSWP forcings produce variations between 0.15 and 2.0 mm/month in ET, surface runoff and subsurface runoff as function of the soil texture map, while WFDE5 produces variations between 7.43 and 9.93 mm/month among soil texture maps. Similar observation was also made for other regions (Tables S1, S2, S4, S5, S6, S7 and S8) and locations (Tables S9, S10, S11, S12, S13, S14, S15 and S16).

575



580 Table 4: Average margin for simulated variables among soil texture maps for GSWP atmospheric forcings (3 hourly), WFDE5 atmospheric forcings (3 hourly) and WFDE5 atmospheric forcings aggregated to hourly resolution over Abuja (mm/month).

Variable	3H-WFDE5	GSWP	WFDE5
Evapotranspiration	2.00	1.33	9.93
Surface Runoff	0.21	0.15	7.43
Subsurface Runoff	0.63	0.41	7.70
Soil Moisture	0.01	0.01	0.01

585 The FAO and SoilGrids soil texture maps, upscaled with different methods and used as input for the CLM5 land surface model, resulted in some cases in different simulated surface runoff, subsurface runoff, and evapotranspiration. In many other cases, simulated runoff and evapotranspiration were not affected by soil texture. Mainly for the WFDE5 forced simulations, with a higher temporal resolution of atmospheric inputs, different soil texture maps (and differently upscaled SoilGrids texture maps) resulted in different simulated surface runoff, subsurface runoff, and evapotranspiration. We investigated therefore whether the higher temporal resolution of those simulations changed rainfall intensity influencing the rainfall partitioning into surface runoff and infiltration.

590 The absolute monthly (Figures S20 and S21) and annual (Figure 2) precipitation amounts over the continent differ somewhat between CRUNCEP, GSWP and WFDE5. The spatial averages for annual precipitation are 608mm/year, 638mm/year and 666mm/year for CRUNCEP, GSWP and WFDE5 respectively. These differences in rainfall amount do not explain why only for WFDE5, soil texture variations result in larger runoff and evapotranspiration variations. We analysed also the number of precipitation events with a rainfall intensity above 3mm/hour for each of the three atmospheric forcings and eight selected locations. WFDE5 had a much higher number of precipitation events with rainfall intensity greater than 3mm/hour than both CRUNCEP and GSWP at all 8 locations (see Table 3). GSWP and CRUNCEP had more rainfall events with much lower intensities. It also indicates that rainfall intensity representation within the model is a likely reason for the higher sensitivity of model outcomes towards soil texture input in WFDE5 forced simulations than GSWP and CRUNCEP forced simulations.

600

Table 5: Total number of precipitation events above 3mm/hour according to CRUNCEP, GSWP and WFDE5 forcings. Also the soil type is provided at each location (gridcell) for FAO, Soilgrids upscaled by dominant selection, SoilGrids upscaled by averaging and SoilGrids upscaled by random selection. SL: sandyloam, SCL: sandyclayloam, L: loam, CL: clayloam, SC: sandyclay, S: sand, C: clay, LS: sandyloam.



Locations	Lon	Lat	CRUN	GSWP	WFDE5	FAO	SGDom	SGMean	SGRand
Salong	20.89	-2.43	0	39	387	SCL	SC	SC	SC
Abuja	7.39	9.07	1	25	234	SL	SCL	SCL	SCL
D. Salaam	39.2	-6.79	7	67	217	L	S	L	L
Maseru	27.48	-29.31	4	23	122	L	CL	CL	CL
Addis	38.75	8.98	4	23	122	C	C	C	C
Windhoek	17.06	-22.56	4	24	75	L	SCL	SCL	SCL
Agadez	7.98	16.97	4	4	37	SL	LS	LS	SL
Cairo	31.23	30.04	0	0	4	L	SL	SL	SCL

605

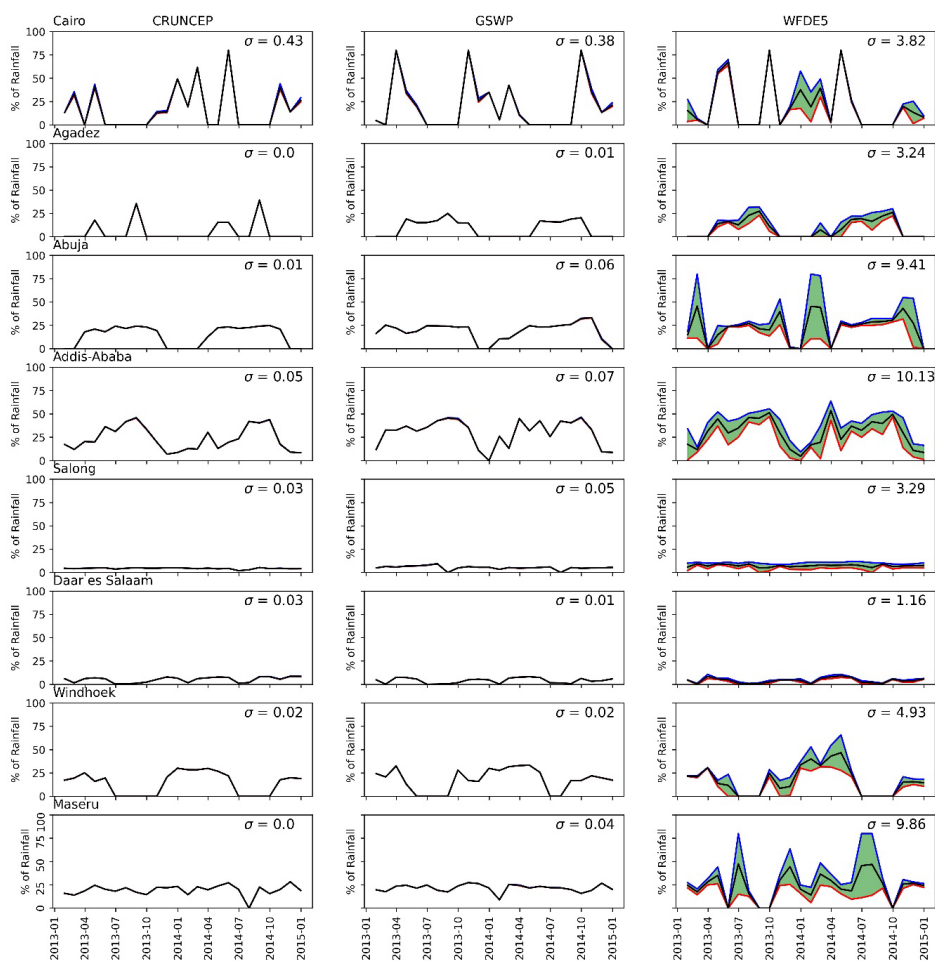
Rainfall intensity has a stronger influence on surface runoff generation than rainfall amount (e.g., Jungerius & ten Harkel, 1994; Yao et al., 2021) and surface runoff is on the other hand also strongly influenced by the hydraulic conductivity with lower conductivity supporting higher surface runoff (Suryatmojo & Kosugi, 2021; Ow & Chow, 2021; Chandler et al., 2018). Therefore, for WFDE5 forcings there are potentially more situations with surface runoff, so that the role of different soil properties can come into play. This is analyzed for all 8 locations (Figure 11) by calculating the standard deviation of the fraction of precipitation turned into surface runoff among the 4 soil texture maps, for each atmospheric forcing. For the WFDE5 atmospheric forcings, this standard deviation is increased with values of 1.16% of rainfall for Daar es Salaam and even 10.13% of rainfall in Addis-Ababa while the standard deviations is less than 0.1% for both CRUNCEP (6 hourly) and GSWP (3 hourly) atmospheric forcings, for all locations except Cairo. Also for Cairo the standard deviation of the precipitation fraction that becomes surface runoff is small for CRUNCEP and GSWP forcing datasets with values around 0.4%. This shows that the soil texture information has a larger control on the partitioning of fluxes for higher temporal resolution atmospheric forcings.

610

615

As surface runoff and infiltration are sensitive to rainfall intensity (Mertens et al., 2002) and soil texture determines saturated hydraulic conductivity and therefore the timing of runoff (Hammond et al., 2019), surface runoff and subsurface runoff vary as a function of soil texture inputs in the WFDE5 simulations (mainly at the local and regional scales).

620



625 **Figure 11: Time series of the standard deviation of percentage of precipitation which turns into surface runoff, across all soil texture maps for eight different locations and three atmospheric forcings. Left column: CRUNCEP, middle column: GSWP and right column: WFDE5. The black line represents the mean, the blue line the maximum percentage of surface runoff for the location, the red line the minimum while the green shade represents deviations from the mean.**

4. Conclusion

630 CLM5 model runs over the African continent were performed at a high spatial resolution of approximately 3km, with four different soil texture maps and three different atmospheric forcings. The four different soil texture inputs included the FAO soil map and three differently upscaled SoilGrids250 maps. The three different atmospheric forcings were CRUNCEPv7, GSWP3 and WFDE5. The most important findings were:

- 635 I. Different soil texture upscaling methods result in different soil texture maps as input for land surface model simulations, but the mean annual evapotranspiration and mean annual surface runoff over Africa are hardly affected by these variations, whereas the mean annual subsurface runoff shows a higher sensitivity with respect to the upscaling method.



- II. The source of soil texture information (FAO versus SoilGrids) exerts a larger impact on simulated ET, surface runoff, subsurface runoff and soil moisture content than the soil texture upscaling method.
- 640 III. The temporal resolution of atmospheric forcings has a minimal effect on the estimated annual evapotranspiration, but significantly influences surface runoff and subsurface runoff. The higher temporal resolution of WFDE5 forcings (hourly) than the other atmospheric forcings resulted in larger variations in simulated ET, surface runoff and subsurface runoff for the different soil texture maps, pointing to the fact that the impact of soil texture becomes more important in combination with higher
- 645 temporal resolution of atmospheric forcings.
- IV. Varying the atmospheric forcings for the land surface model impacts the simulation of actual ET more than varying the soil texture input.

This work focused on differences in simulation results as function of different soil texture and atmospheric inputs and the interaction between the temporal resolution of the atmospheric forcings and soil texture. It is assumed in

650 this work that model shortcomings (for example related to the representation of yearly vegetation cycles and the representation of different crop types) do not affect substantially the differences in the simulation results. Furthermore, the release of CLM5 used in this work assumes 16 plant functional types for the African continent by default which does not represent all vegetation types. Also, irrigation is hardcoded into the surface datasets. Future work should reduce these limitations.

655

Data Availability

This study only uses publicly available data sources, and they were cited wherever applicable. Summary tables indicating average margin for simulated variables among soil texture maps for GSWP, WFDE5 (3 hourly) and WFDE5 (hourly) as calculated are included in the supplement. The coordinates for partitioning Africa into 8

660 regions as done in this study were also cited where applicable.

Author Contribution

Bamidele Oloruntoba: Data curation, Methodology, Formal analysis, Investigation, Software, Visualization, Writing – original draft preparation. Stefan Kollet: Conceptualization, Methodology, Writing – review & editing. Carsten Montzka: Conceptualization, Methodology, Writing – review & editing. Harry Vereecken: Conceptualization, Methodology, Writing – review & editing. Harrie-Jan Hendricks Franssen: Conceptualization, Methodology, Supervision, Writing – review & editing.

665

Competing Interests

At least one of the (co-)authors is a member of the editorial board of Hydrology and Earth System Sciences.



References

- 670 Bonan, G. B., Lombardozi, D. L., Wieder, W. R., Oleson, K. W., Lawrence, D. M., Hoffman, F. M., and Collier, N.: Model Structure and Climate Data Uncertainty in Historical Simulations of the Terrestrial Carbon Cycle (1850–2014), *Glob. Biogeochem. Cycles*, 33, 1310–1326, <https://doi.org/10.1029/2019GB006175>, 2019.
- Bouilloud, L., Chancibault, K., Vincendon, B., Ducrocq, V., Habets, F., Saulnier, G.-M., Anquetin, S., Martin, E., and Noilhan, J.: Coupling the ISBA Land Surface Model and the TOPMODEL Hydrological Model for Mediterranean Flash-Flood Forecasting: Description, Calibration, and Validation, *J. Hydrometeorol.*, 11, 315–333, <https://doi.org/10.1175/2009JHM1163.1>, 2010.
- 675 Boucchignani, E., Cattaneo, L., Panitz, H.-J., and Mercogliano, P.: Sensitivity analysis with the regional climate model COSMO-CLM over the CORDEX-MENA domain, *Meteorol. Atmospheric Phys.*, 128, 73–95, <https://doi.org/10.1007/s00703-015-0403-3>, 2016.
- 680 Chandler, K. R., Stevens, C. J., Binley, A., and Keith, A. M.: Influence of tree species and forest land use on soil hydraulic conductivity and implications for surface runoff generation, *Geoderma*, 310, 120–127, <https://doi.org/10.1016/j.geoderma.2017.08.011>, 2018.
- Compo, G. P., Whitaker, J. S., Sardeshmukh, P. D., Matsui, N., Allan, R. J., Yin, X., Gleason, B. E., Vose, R. S., Rutledge, G., Bessemoulin, P., Brönnimann, S., Brunet, M., Crouthamel, R. I., Grant, A. N., Groisman, P. Y., Jones, P. D., Kruk, M. C., Kruger, A. C., Marshall, G. J., Mauerer, M., Mok, H. Y., Nordli, Ø., Ross, T. F., Trigo, R. M., Wang, X. L., Woodruff, S. D., and Worley, S. J.: The Twentieth Century Reanalysis Project, *Q. J. R. Meteorol. Soc.*, 137, 1–28, <https://doi.org/10.1002/qj.776>, 2011.
- 685 Cosby, B. J., Hornberger, G. M., Clapp, R. B., and Ginn, T. R.: A Statistical Exploration of the Relationships of Soil Moisture Characteristics to the Physical Properties of Soils, *Water Resour. Res.*, 20, 682–690, <https://doi.org/10.1029/WR020i006p00682>, 1984.
- Cocchi, M., Weedon, G. P., Amici, A., Bellouin, N., Lange, S., Schmied, H. M., Hersbach, H., and Buontempo, C.: WFDE5: bias adjusted ERA5 reanalysis data for impact studies, *Earth Syst. Sci. Data Discuss.*, 1–32, <https://doi.org/10.5194/essd-2020-28>, 2020.
- 695 Dai, Y., Shangguan, W., Wei, N., Xin, Q., Yuan, H., Zhang, S., Liu, S., Lu, X., Wang, D., and Yan, F.: A review of the global soil property maps for Earth system models, *SOIL*, 5, 137–158, <https://doi.org/10.5194/soil-5-137-2019>, 2019.
- Dube, T., Seaton, D., Shoko, C., and Mbow, C.: Advancements in earth observation for water resources monitoring and management in Africa: A comprehensive review, *J. Hydrol.*, 623, 129738, <https://doi.org/10.1016/j.jhydrol.2023.129738>, 2023.
- 700 Ghent, D., Kaduk, J., Remedios, J., Ardö, J., and Balzter, H.: Assimilation of land surface temperature into the land surface model JULES with an ensemble Kalman filter, *J. Geophys. Res. Atmospheres*, 115, <https://doi.org/10.1029/2010JD014392>, 2010.
- Global Soil Data Task: Global Soil Data Products CD-ROM Contents (IGBP-DIS), ORNL DAAC, <https://doi.org/10.3334/ORNLDAAC/565>, 2014.
- 705 Hammond, J. C., Harpold, A. A., Weiss, S., and Kampf, S. K.: Partitioning snowmelt and rainfall in the critical zone: effects of climate type and soil properties, *Hydrol. Earth Syst. Sci.*, 23, 3553–3570, <https://doi.org/10.5194/hess-23-3553-2019>, 2019.
- Harris, I.: CRU TS3.21: Climatic Research Unit (CRU) Time-Series (TS) Version 3.21 of High Resolution Gridded Data of Month-by-month Variation in Climate (Jan. 1901 - Dec. 2012) (3.21), <https://doi.org/10.5285/D0E1585D-3417-485F-87AE-4FCECF10A992>, 2013.
- 710 Hengl, T., Jesus, J. M. de, Heuvelink, G. B. M., Gonzalez, M. R., Kilibarda, M., Blagotić, A., Shangguan, W., Wright, M. N., Geng, X., Bauer-Marschallinger, B., Guevara, M. A., Vargas, R., MacMillan, R. A., Batjes, N. H., Leenaars, J. G. B., Ribeiro, E., Wheeler, I., Mantel, S., and Kempen, B.: SoilGrids250m: Global gridded soil



- 715 information based on machine learning, *PLOS ONE*, 12, e0169748, <https://doi.org/10.1371/journal.pone.0169748>, 2017.
- Hengl, T., Miller, M. A. E., Krizán, J., Shepherd, K. D., Sila, A., Kilibarda, M., Antonijević, O., Glušica, L., Dobermann, A., Haefele, S. M., McGrath, S. P., Acquah, G. E., Collinson, J., Parente, L., Sheykhmousa, M., Saito, K., Johnson, J.-M., Chamberlin, J., Silatsa, F. B. T., Yemefack, M., Wendt, J., MacMillan, R. A., Wheeler, I., and Crouch, J.: African soil properties and nutrients mapped at 30 m spatial resolution using two-scale ensemble machine learning, *Sci. Rep.*, 11, 6130, <https://doi.org/10.1038/s41598-021-85639-y>, 2021.
- 720
- Huber, S., Fensholt, R., and Rasmussen, K.: Water availability as the driver of vegetation dynamics in the African Sahel from 1982 to 2007, *Glob. Planet. Change*, 76, 186–195, <https://doi.org/10.1016/j.gloplacha.2011.01.006>, 2011.
- Hyungjun, K.: Global Soil Wetness Project Phase 3 Atmospheric Boundary Conditions (Experiment 1), 5, <https://doi.org/doi:10.20783/DIAS.501>, 2017.
- 725
- Iturbide, M., Gutiérrez, J. M., Alves, L. M., Bedia, J., Gimeno, E., Cofiño, A. S., Cerezo-Mota, R., Di Luca, A., Faria, S. H., Gorodetskaya, I., Hauser, M., Herrera, S., Hewitt, H. T., Hennessy, K. J., Jones, R. G., Krakovska, S., Manzanar, R., Martínez-Castro, D., Narisma, G. T., Nurhati, I. S., Pinto, I., Seneviratne, S. I., van den Hurk, B., and Vera, C. S.: An update of IPCC climate reference regions for subcontinental analysis of climate model data: Definition and aggregated datasets, *Data, Algorithms, and Models*, <https://doi.org/10.5194/essd-2019-258>, 2020.
- 730
- Kalnay, E., Kanamitsu, M., Kistler, R., Collins, W., Deaven, D., Gandin, L., Iredell, M., Saha, S., White, G., Woollen, J., Zhu, Y., Leetmaa, A., Reynolds, B., Chelliah, M., Ebisuzaki, W., Higgins, W., Janowiak, J., Mo, K. C., Ropelewski, C., Wang, J., Jenne, R., and Joseph, D.: The NCEP/NCAR 40-Year Reanalysis Project, *Bull. Am. Meteorol. Soc.*, 77, 437–472, [https://doi.org/10.1175/1520-0477\(1996\)077<0437:TNYRP>2.0.CO;2](https://doi.org/10.1175/1520-0477(1996)077<0437:TNYRP>2.0.CO;2), 1996.
- 735
- Kochendorfer, J. P. and Ramírez, J. A.: Ecohydrologic controls on vegetation density and evapotranspiration partitioning across the climatic gradients of the central United States, *Hydrol. Earth Syst. Sci.*, 14, 2121–2139, <https://doi.org/10.5194/hess-14-2121-2010>, 2010.
- 740
- Lawrence, D., Fisher, R., Koven, C., Oleson, K., Swenson, S., Vertenstein, M., Andre, B., Bonan, G., Ghimire, B., Kennedy, D., Kluzek, E., Knox, R., Lawrence, P., Li, F., Li, H., Lombardozzi, D., Lu, Y., Peket, J., Riley, W., and Xu, C.: CLM5.0 Technical Description, 2018.
- Lawrence, D. M., Fisher, R. A., Koven, C. D., Oleson, K. W., Swenson, S. C., Bonan, G., Collier, N., Ghimire, B., Kampenhout, L. van, Kennedy, D., Kluzek, E., Lawrence, P. J., Li, F., Li, H., Lombardozzi, D., Riley, W. J., Sacks, W. J., Shi, M., Vertenstein, M., Wieder, W. R., Xu, C., Ali, A. A., Badger, A. M., Bisht, G., Broeke, M. van den, Brunke, M. A., Burns, S. P., Buzan, J., Clark, M., Craig, A., Dahlin, K., Drewniak, B., Fisher, J. B., Flanner, M., Fox, A. M., Gentine, P., Hoffman, F., Keppel-Aleks, G., Knox, R., Kumar, S., Lenaerts, J., Leung, L. R., Lipscomb, W. H., Lu, Y., Pandey, A., Pelletier, J. D., Perket, J., Randerson, J. T., Ricciuto, D. M., Sanderson, B. M., Slater, A., Subin, Z. M., Tang, J., Thomas, R. Q., Martin, M. V., and Zeng, X.: The Community Land Model Version 5: Description of New Features, Benchmarking, and Impact of Forcing Uncertainty, *J. Adv. Model. Earth Syst.*, 11, 4245–4287, <https://doi.org/10.1029/2018MS001583>, 2019.
- 745
- 750
- Li, L., Bisht, G., and Leung, L. R.: Spatial heterogeneity effects on land surface modeling of water and energy partitioning, *Geosci. Model Dev.*, 15, 5489–5510, <https://doi.org/10.5194/gmd-15-5489-2022>, 2022.
- Lovat, A., Vincendon, B., and Ducrocq, V.: Assessing the impact of resolution and soil datasets on flash-flood modelling, *Hydrol. Earth Syst. Sci.*, 23, 1801–1818, <https://doi.org/10.5194/hess-23-1801-2019>, 2019.
- 755
- Mertens, J., Raes, D., and Feyen, J.: Incorporating rainfall intensity into daily rainfall records for simulating runoff and infiltration into soil profiles, *Hydrol. Process.*, 16, 731–739, <https://doi.org/10.1002/hyp.1005>, 2002.
- Myeni, L., Moeletsi, M. E., and Clulow, A. D.: Present status of soil moisture estimation over the African continent, *J. Hydrol. Reg. Stud.*, 21, 14–24, <https://doi.org/10.1016/j.ejrh.2018.11.004>, 2019.



- 760 Pelletier, J. D., Broxton, P. D., Hazenberg, P., Zeng, X., Troch, P. A., Niu, G.-Y., Williams, Z., Brunke, M. A., and Gochis, D.: A gridded global data set of soil, intact regolith, and sedimentary deposit thicknesses for regional and global land surface modeling, *J. Adv. Model. Earth Syst.*, 8, 41–65, <https://doi.org/10.1002/2015MS000526>, 2016.
- 765 Reynolds, C. A., Jackson, T. J., and Rawls, W. J.: Estimating soil water-holding capacities by linking the Food and Agriculture Organization Soil map of the world with global pedon databases and continuous pedotransfer functions, *Water Resour. Res.*, 36, 3653–3662, <https://doi.org/10.1029/2000WR900130>, 2000.
- Schneider, U., Becker, A., Finger, P., Meyer-Christoffer, A., Ziese, M., and Rudolf, B.: GPCC’s new land surface precipitation climatology based on quality-controlled in situ data and its role in quantifying the global water cycle, *Theor. Appl. Climatol.*, 115, 15–40, <https://doi.org/10.1007/s00704-013-0860-x>, 2014.
- 770 Tafasca, S., Ducharme, A., and Valentin, C.: Weak sensitivity of the terrestrial water budget to global soil texture maps in the ORCHIDEE land surface model, *Hydrol. Earth Syst. Sci. Discuss.*, 1–20, <https://doi.org/10.5194/hess-2019-305>, 2019.
- 775 Traore, A. K., Ciais, P., Vuichard, N., Poulter, B., Viovy, N., Guimberteau, M., Jung, M., Myneni, R., and Fisher, J. B.: Evaluation of the ORCHIDEE ecosystem model over Africa against 25 years of satellite-based water and carbon measurements, *J. Geophys. Res. Biogeosciences*, 119, 1554–1575, <https://doi.org/10.1002/2014JG002638>, 2014.
- Vahmani, P. and Hogue, T. S.: High-resolution land surface modeling utilizing remote sensing parameters and the Noah UCM: a case study in the Los Angeles Basin, *Hydrol. Earth Syst. Sci.*, 18, 4791–4806, <https://doi.org/10.5194/hess-18-4791-2014>, 2014.
- 780 Viovy, N.: CRUNCEP Version 7 - Atmospheric Forcing Data for the Community Land Model, <https://doi.org/10.5065/PZ8F-F017>, 2018.
- Weber, U., Jung, M., Reichstein, M., Beer, C., Braakhekke, M. C., Lehsten, V., Ghent, D., Kaduk, J., Viovy, N., Ciais, P., Gobron, N., and Rodenbeck, C.: The interannual variability of Africa’s ecosystem productivity: a multi-model analysis, 11, 2009.
- 785 Weedon, G. P., Balsamo, G., Bellouin, N., Gomes, S., Best, M. J., and Viterbo, P.: The WFDEI meteorological forcing data set: WATCH Forcing Data methodology applied to ERA-Interim reanalysis data, *Water Resour. Res.*, 50, 7505–7514, <https://doi.org/10.1002/2014WR015638>, 2014.
- Xu, C., Torres-Rojas, L., Vergopolan, N., and Chaney, N. W.: The Benefits of Using State-Of-The-Art Digital Soil Properties Maps to Improve the Modeling of Soil Moisture in Land Surface Models, *Water Resour. Res.*, 59, e2022WR032336, <https://doi.org/10.1029/2022WR032336>, 2023.
- 790 Yoshimura, K. and Kanamitsu, M.: Dynamical Global Downscaling of Global Reanalysis, *Mon. Weather Rev.*, 136, 2983–2998, <https://doi.org/10.1175/2008MWR2281.1>, 2008.
- Zhao, H., Zeng, Y., Lv, S., and Su, Z.: Analysis of soil hydraulic and thermal properties for land surface modeling over the Tibetan Plateau, *Earth Syst. Sci. Data*, 10, 1031–1061, <https://doi.org/10.5194/essd-10-1031-2018>, 2018.
- 795 A world soil hydrology file for global climate modeling, Technical Memorandum 87802: <https://data.giss.nasa.gov/landuse/soilunit.html>, last access: 18 February 2021.